

ESTIMATING THE MOST LIKELY EXTREME NACELLE ACCELERATION OF A FLOATING OFFSHORE WIND TURBINE FROM PHYSICAL MODEL TANK TESTING

Ailsa McMillan^{1,2,*}, Prof. Alasdair McDonald², Dr. Ajit C. Pillai³, Dr. Zhiming Yuan⁴, Dr. Thomas Davey¹

¹FloWave Ocean Energy Research Facility, Edinburgh, United Kingdom

²University of Edinburgh, Edinburgh, United Kingdom

³University of Exeter, Penryn, United Kingdom

⁴University of Strathclyde, Glasgow, United Kingdom

ABSTRACT

The floating platforms on which floating offshore wind turbines are mounted introduce considerable complexity in terms of dynamic motion. Understanding the extreme response of these marine structures is important. One such extreme response is the nacelle accelerations, which can cause damage to nacelle components, such as the generator, and should therefore be kept to a minimum. Tank testing is a tool which can be used to understand the behaviour of these structures, and to determine extreme response. Here, a method of estimating the most likely extreme nacelle accelerations from a tank testing programme is shown, using a 1:100 scaled model of the IEA 15 MW turbine with the Voltorn-US semi-submersible platform. The results showed that the most likely extreme nacelle accelerations within the chosen 50-year return sea state are 0.195 g in the fore-aft direction, with a typical safety limit of 0.2-0.4 g. Extreme statistical analysis was carried out on the data obtained by a 3-DOF accelerometer, using the peaks-over-threshold (POT) method fitted to a generalised Pareto distribution (GPD). Threshold selection and declustering of data are also discussed. The results may be applied to further test programmes, aiding in the development and design of current or novel floating platforms in any programmable sea state.

Keywords: floating wind turbines, tank testing, peaks-over-threshold, generalised Pareto distribution, extreme statistics, extreme waves

1. INTRODUCTION

Floating offshore wind turbines (FOWTs) are increasingly being installed globally. Scaled experiments in wave tanks are a strategy for testing these devices, allowing for programmable and repeatable sea states and numerical model validation without incurring the costs of full-scale testing. Introducing a float-

ing platform and mooring system to offshore wind turbines has introduced complex dynamic motion from the combined wind, wave, and current loads. FOWTs are typically mounted on semi-submersible, spar-buoy, tension leg platform (TLP), or barge-type floaters, where many of the platform designs have been used in oil and gas [1, 2]. The concept of adding wind turbines to the floating platform would not have been in the initial design considerations of the platform. However, tank testing can be further used to indicate the suitability of using these platforms for wind turbines, and/or the development of novel floater concepts specifically for the purpose of floating wind.

A key use of tank testing results is for the development and validation of numerical models for FOWTs, such as OpenFAST [3, 4]. One instance where numerical models can diverge from physical testing results is during extreme events, where the integration schemes and model stability can begin to fail for the more complex environments associated with extremes [5, 6]. Testing extreme conditions is vital in demonstrating that components of the turbine can survive the conditions that they are exposed to, as well as for certification and insurance.

Many parameters can be obtained using tank testing, including the accelerations that are experienced by the nacelle. The nacelle houses key components of the wind turbine, such as the generator and control systems. When nacelle acceleration limits are exceeded, this could result in degradation of turbine performance and damage to drive train equipment [7]. Therefore, keeping nacelle accelerations to a minimum should be an important design consideration. Failure modes of existing floating offshore farms are often not publically available, but it is likely that nacelle accelerations are at least of interest. The design limits of nacelle accelerations for the turbine are generally considered to be 0.2-0.4 g [8, 9]. This value changes depending on parameters such as the turbine manufacturer, and the turbine rating. By using statistical methods, understanding whether it is likely

*Corresponding author: A.C.McMillan-1@sms.ed.ac.uk
Documentation for asmeconf.cLs: Version 1.35, March 22, 2024.

that the nacelle accelerations may be exceeded could be useful in determining the survival of the turbine in extreme conditions, and may be able to feed into design to adapt them to further limit these accelerations, or inform developers about the likelihood of an operation and maintenance task being required after certain conditions have been reached.

For extreme conditions, such as significant wave height, and wind speeds, statistical methods such as the peaks-over-threshold (POT) method can be used to identify the frequency that threshold value is exceeded. The generalised Pareto distribution (GPD) is then used to fit the exceedance data. Threshold selection and declustering of data is an important consideration in this work. FOWTs are being located in more and more sites across the world, with very different conditions, and as such, it is important to understand the site-specific nacelle accelerations to ensure that the platform choice is suitable. The method of obtaining the acceleration from a tank testing programme using a 3-DOF accelerometer placed on the nacelle, as well as how the statistical methods mentioned will be applied to the data presents the return value nacelle acceleration, and determines if the floating wind turbine would be likely to exceed typical nacelle acceleration safety limits. Exceeding these values may result in turbine failure, which would result in increased operation and maintenance costs, and potential downtime, resulting in lost revenue. If nacelle acceleration limits are likely to be exceeded in extreme sea states, further design optimisation should be considered. The paper is structured in two parts, the physical model testing, followed by the statistical analysis and discussion.

2. METHODS

2.1 Experimental Methods

Nacelle accelerations were obtained by tests using a 1:100 Froude scaled model of the IEA 15 MW reference turbine with the Voltorn-US Semisubmersible platform [10]. The scaled model has been designed by FloWave Ocean Energy Research Facility (known as FloWave herein) and tests were carried out in the Curved Wave Tank facility at the University of Edinburgh (Figure 1).

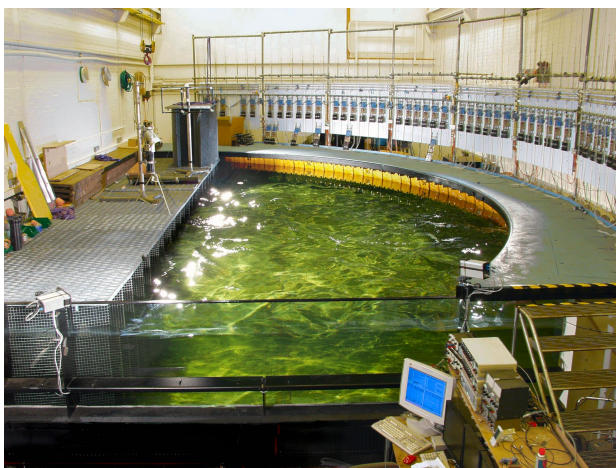


FIGURE 1: THE CURVED WAVE TANK FACILITY AT THE UNIVERSITY OF EDINBURGH, SCOTLAND

The tank is shaped in an arc, and comprises 48 force feedback absorbing wavemakers in a 9 m arc. The tank depth is 1.15 m, and is capable of uni- and multi-directional sea states.

2.1.1 Model Properties. The model properties, material properties, and mooring properties are defined in Tables 1 and 2 respectively.

TABLE 1: MODEL PROPERTIES

Parameter	Value
Total mass	21.1 kg
Draft	0.20 m
Nacelle mass	0.86 kg
Moments of inertia [kgm^2]	[4.62, 4.62, 2.36]

The optimal spring type and arrangement were selected using an in-house FloWave design method that aims to accurately scale the mooring stiffness matrix. Six springs were arranged in series on each line to achieve the scaled line stiffness. The mooring properties are described in Table 2.

TABLE 2: MOORING PROPERTIES

Parameter	Value
Number of mooring lines	3
Declination angle	65°
Pretension	1.16 N
Min force	0.22 N
Max force	3.08 N
Max travel	0.38 m
Line axial stiffness	5 N/m

2.1.2 Tank Set-Up. A rope-spring system has been utilised, with the springs being used to introduce line compliance. These were mounted at the tank edge side, to avoid their weight impacting the hydrodynamics of the line at the model side. The load cell was mounted at the fairlead attachment point on the model. This setup is shown in Figures 2 and 3.

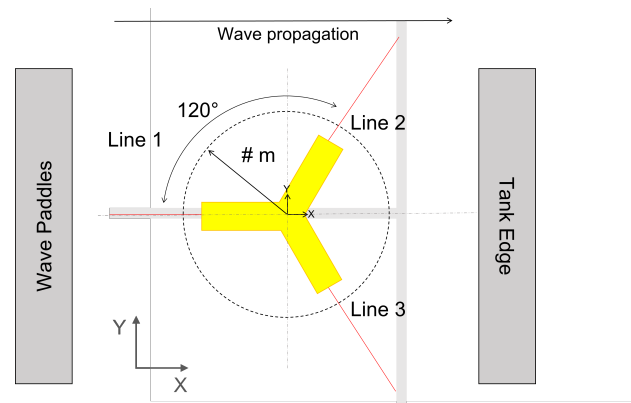


FIGURE 2: DIAGRAM OF THE TANK SET UP FROM THE XY VIEW, ADAPTED FROM [11]

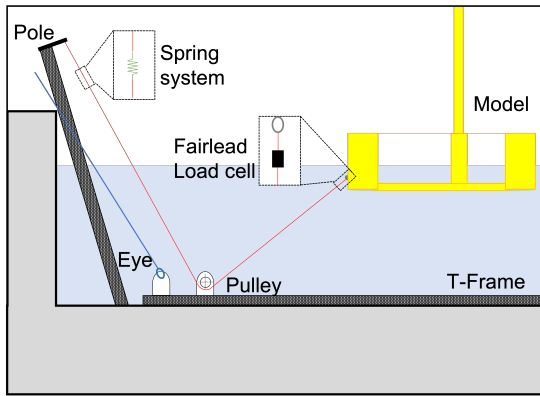


FIGURE 3: DIAGRAM OF THE TANK SET UP FROM THE XZ VIEW

All required instrumentation was calibrated within three days of the test programme, with refinement or full calibrations carried out each day of testing where appropriate. The 3-DOF accelerometer used does not require calibration, and scaling was added to the results by the manufacturer’s recommendation. The accelerometer was checked by ensuring that each degree of freedom read 1g when positioned on the respective axis. The nacelle has been designed to account for the weight of the accelerometer and has been placed such that the accelerometer is in line with $x, y[0, 0]$. A nacelle was 3D printed with carbon fibre, with a slot for the accelerometer to be in line with the centre line of the turbine tower. The weight of the nacelle was then made up to the target weight with aluminium plates, distributed evenly.

The accelerometer data was obtained by using a DAQ system connected to LabVIEW Software. The accelerometer can give measurements in 3-DOF. The data set was centred around zero by subtracting the mean of the data set. Subsequently, the absolute values of the data was computed for amplitude-focused analysis.

2.1.3 Sea States. The sea state that was chosen was adapted from the IEC Design Load Case Matrix in [12] and is presented in Table 3.

TABLE 3: TARGET AND OBSERVED EXTREME SEA STATES

	Significant Wave Height (m)	Peak Period (s)	Gamma Shape Factor (-)
Full scale	10.7	14.2	2.75
1:100 scale	0.107	1.42	2.75
Tank output	0.104	1.42	2.75

In offshore wind engineering, the 50-year significant wave height is a critical design parameter and is referred to in standards and guidance such as the IEC 61400-3 and American Bureau of Shipping (ABS) as an extreme condition [12, 13]. The 50-year return period represents the most probable extreme condition expected to occur within a 50-year timeframe, often determined using statistical techniques such as the inverse first order reliability method (IFORM) [12]. The 50-year return period was taken and was scaled down to a 1:100 scale using Froude scaling.

As shown in Table 3, the sea states generated by the Curved

Wave Tank have not been corrected to match the sea states of the design load case matrix at 1:100 scale. Corrected values are not required for this specific research, as the present research concentrates on the methods of obtaining the statistical analysis from tank testing results, and the tank testing programme can be altered as required. The 50-year return period case load estimates the most extreme sea state that will occur in a 50-year period using statistical methods. In extreme testing, the standards are to test these sea states for three hours or equivalent, which equates to approximately 1000 waves. At 1:100 scale, following Froude scaling, this equates to 18 minutes at the tank scale. The sea state was run for 20 and a half minutes to allow for tank ramp-up time, with data from the first thirty seconds being removed in post-processing. The extra minutes were a precautionary measure to ensure the attainment of approximately 1000 waves. Herein, the mean of the data will refer to the mean of the absolute value of the data post-processing and data cleaning.

3. ANALYTICAL METHODS

The method is summarised below:

1. Data cleaning,
2. Select an appropriate threshold,
3. Apply the threshold to data,
4. Apply a zero-up crossing approach to determine peaks above threshold,
5. Use the MATLAB 'Distribution Fitter' to fit a GPD to the identified peaks in the data.

These points will be expanded on in the proceeding subsections.

3.1 Selection of probability model

Statistical methods have been used to obtain information about extremes in datasets for decades (e.g. see Davenport [14]). Notable examples of areas where extreme values are of importance are in hydrology and finance as well as in engineering, with examples found in [15–17]. Many examples of research use extreme statistics to determine the most likely extreme significant wave height, associated period, and wind speed [18–20]. Historically, the extremes of wind speeds have been estimated by and fitted using Gumbel, or Weibull distributions, which are two probability distributions associated with extreme values [21]. The generalised extreme value (GEV) distribution may also be used which involves combining the Gumbel, Frechet, and Weibull distributions (also known as Types I, II, and III respectively) [22]. Typically, values from an annual block maximum are used in data sets fitted to this kind of distribution. However, limitations of this include the possibility of leaving too few data points to have an appropriate fit unless there are many years of good data. Additionally, it can eliminate extreme values that may otherwise bear importance to the analysis that occurred throughout the year but was not the absolute maximum [22]. For example, it is estimated that approximately 160 independent extreme events happen annually for waves [23]. A more recent method of estimating the

extreme values is the peaks-over-threshold (POT) method, also known as the partial-duration-series (PDS), which involves applying an appropriate threshold to the data, and fitting a distribution to the data points that exceeds this threshold. The chosen distribution was the GPD, which is associated to the POT method in works such as [18, 24–26]. Viselli et al. [18], analysed identical data sets using the GEV, and the POT method, and found that the GEV methods using block maxima consistently predicted larger values. Mackay et al. [19], show that neglecting serial correlation in models can lead to a positive bias. This is evidence of a trade-off, as the method requires the points to be independent, and therefore not correlated to each other, however, by using blocks of a large size, lots of information is lost and can therefore lead to overestimation. The GPD was used in this work, which is a family of continuous probability distributions. It is often used in modelling the tails of distributions, and therefore frequently used for extreme analysis. The distribution is generally defined by a shape (ξ), scale (σ) and in some instances a location parameter for data that exceeds a specified threshold (μ). The cumulative distribution function (CDF) of the GPD can be defined mathematically as follows in Equations 1 and 2.

$$H(y) = 1 - \left(1 + \xi \left(\frac{\xi y}{\tilde{\sigma}}\right)\right)^{-\frac{1}{\xi}} \quad (1)$$

Where:

$$\tilde{\sigma} = \sigma + \xi(u - \mu) \quad (2)$$

Where σ and ξ are the scale and shape parameters respectively that have been estimated for the GPD, u is the threshold and μ is the location parameter [22]. The parameter y is the independent variable of the distribution and could represent any nacelle acceleration. In this work, y represents the accelerations at the nacelle in the fore-aft direction.

3.2 Determination of Appropriate Threshold

Selecting an appropriate threshold for the POT analysis is an important aspect of using the GPD, and is a trade-off between variance and bias [22]. The choice in threshold can have a significant impact on statistics and shape distribution of the data set [27]. If the threshold is too high, too few data points will be generated for the model to be accurately fit, and high variance is seen as a result [22]. If the threshold is too low, then the statistics will no longer provide an accurate representation of the extreme population. It is important to ensure that the most statistically relevant data remains in the distribution as far as possible.

Moriarty et al. [27] used probabilistic methods to determine an optimum threshold in their work looking at fatigue loading in wind turbines. This was determined to be the mean of the data set plus 1.4 times the standard deviation [27]. Authors have adopted this practice in their studies such as [28], however, even Moriarty et al. [27] declared that more sophisticated methods for determining the threshold could be developed in future studies.

The method adopted by Coles et al. [22] is to plot the mean residual life plot and determine if this is linear, which would indicate that the threshold is an appropriate level in which to fit the GPD. In order to obtain the mean residual life plot, the excess of means is first calculated using Equation 3 [22]. In order

to calculate the mean excesses, 100 iterations of the calculation evenly ranging from 0.2 to 5 times the standard deviation of the data plus the mean was taken as the threshold parameter. These parameters are obtained from the result of the tank testing programme. For each iteration of the loop, the scale and shape parameters of the GPD were estimated using the 'gpfir' function in MATLAB, based on the peaks of the data as calculated by up-crossing code that will be further discussed in Section 3.3.

$$E(X - u | X > u) = \frac{\sigma_{u0} + \xi u}{1 - \xi} \quad (3)$$

Where σ_{u0} is the scale parameter at the minimum threshold by which you can fit a GPD, ξ is the shape parameter, and u is the threshold that is being investigated [22].

Further on to this, a mean residual life plot can be derived using Equation 4. This looks at the mean values of the exceedences by looping through a series of threshold values. This can then be again plotted against the threshold values themselves.

$$\left\{ \left(u, \frac{1}{n_u} \sum_{i=1}^{n_u} (x_{(i)} - u) \right) : u < x_{max} \right\} \quad (4)$$

3.3 Declustering of Peaks

The POT/GPD method assumes that the data points in the data set are independent from each other and identically distributed [22]. Extreme values can have a tendency to cluster, meaning they occur concurrently, and as such it can be necessary to perform some analysis in order to decluster them [25]. This clustering effect can lead to serial correlation, where the data points are no longer truly independent of each other which would violate the conditions of the statistical model used. To do this, here the event is defined as the maximum measurement between two concurrent points where the signal crosses the threshold in an upward trajectory, or a 'zero up-crossing method'. This is often applied to wave theory in order to determine the mean wave period of irregular and random waves. This was a more suitable method than using MATLAB's built-in "findpeaks" function for where the data points exceed the threshold. The function locates local maxima, defined as a 'data sample that is larger than its two neighbouring samples or is equal to Inf' [29]. This means that many unintended peaks can be found within a signal, as highlighted in Figure 4, even when the data has been "smoothed".

Other methods used has been to use time windows e.g. 4 or 8 day time windows as presented by Viselli et al [18]. This approach differs with the block maxima approach through the 'characterisation of an observation as extreme if it exceeds a high threshold' [22].

Analysis was performed on the peaks identified by the code. To fit the GPD to the obtained data above the selected threshold, the MATLAB 'Distribution Fitter' application was used, which uses the "gpfir" MATLAB function to estimate the scale and shape parameters.

3.4 Calculation of Return Value

The key aim of this study is to determine whether the most likely extreme nacelle acceleration will exceed 0.2 g, as most safety limits of nacelle acceleration is between 0.2 - 0.4 g.

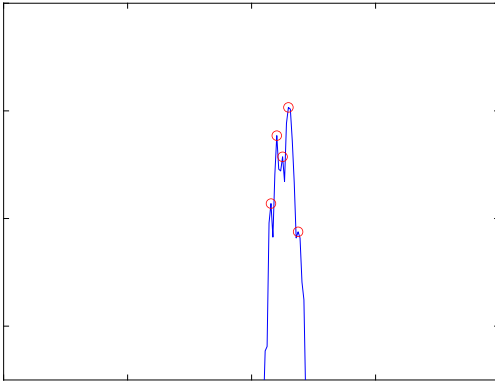


FIGURE 4: AN EXAMPLE OF AN EXTREME EVENT USING 'FINDPEAKS' FUNCTION

In order to obtain a value that can be compared with safety values of the nacelle, the return value must be calculated.

Return values are typically reported in terms of years. However, in this work, the sea state of a 50-year return period has been simulated for approximately 1000 waves. The absolute values of the accelerations scale up 1:1 in Froude scaling to full-scale and so the reported values correlate with full-scale testing. The return value can be calculated using Equation 5.

$$x_m = u + \frac{\sigma}{\xi} [(m\zeta_u)^\xi - 1],$$

where x_m is the return level, u is the threshold set for the analysis, ξ is the shape parameter estimated for the GPD, σ is the scale parameter estimated for the GPD, and ζ_u is the $Pr\{X \leq u\}$ where X is a random variable and is taken as the absolute value of the full data set. m is the number of observations which are taken to be number of peaks and troughs found when applying the zero crossing code to the time series in Figure 5. This is done in order to ensure compliance with the GPD requirement that observations must be independent.

4. RESULTS AND DISCUSSION

4.1 Experimental Nacelle Accelerations Results

The results from the experimental tests for the 20-m extreme sea state in each degree of freedom are as follows in Table 4.

TABLE 4: NACELLE ACCELERATION RESULTS

Parameter	Fore-aft	Side-to-side	Vertical
Mean	0.031	0.0032	0.02
Standard deviation	0.038	0.0040	0.028
Maximum	0.170	0.0329	0.130

From the data set obtained from the tank tests, the fore-aft direction was the most significant, and as such, the data was carried out for this direction. It is likely that different components in the nacelle will have more significant impacts from nacelle

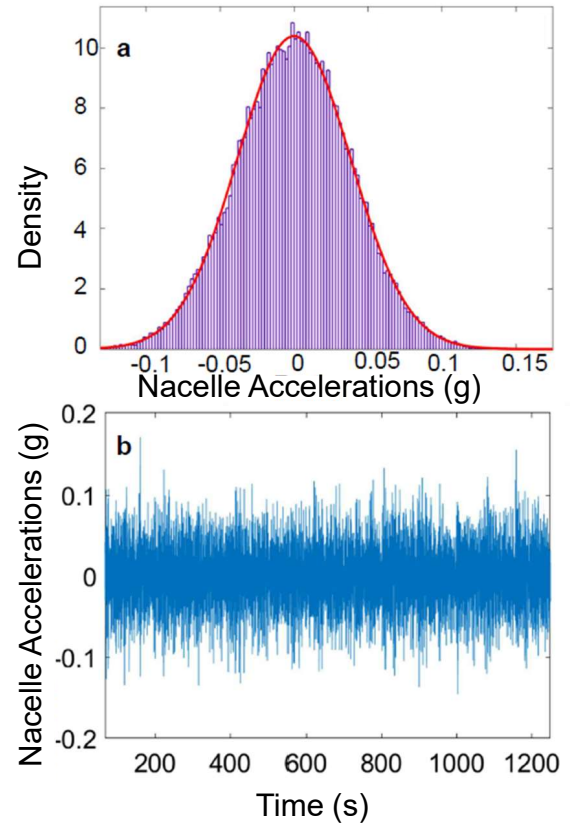


FIGURE 5: THE HISTOGRAM OF THE ZERO MEAN CENTRED DATA RESULTS OF THE ACCELERATIONS (g), WITH THE RED LINE FOLLOWING THE NORMAL DISTRIBUTION AND THE PURPLE HISTOGRAM SHOWING THE DATA (A) AND THE TIME SERIES OF NACELLE ACCELERATIONS IN THE FORE-AFT DIRECTION (B)

The following analysis takes the absolute value of these results and looks at the tails of the distribution.

4.2 Threshold Selection

As shown in Figure 6, there are many points above the threshold. This threshold used in this figure is the mean plus standard deviation multiplied by 1.4, as shown in Moriarty et al and discussed in previous sections [27]. Inspection by eye can quickly indicate that the threshold appears to be too low using this value, and further analysis must be carried out in order to determine the appropriate threshold.

As outlined in the methods, the mean excesses and mean residuals plot are presented in Figures 7 and 8. The mean resid-

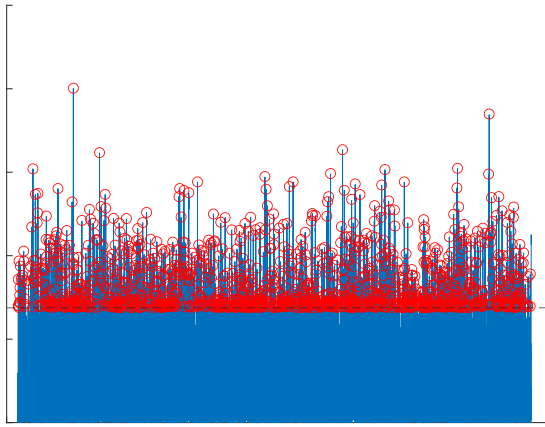


FIGURE 6: THE POT GRAPH USING THE THRESHOLD RECOMMENDED BY MORIARTY ET AL [27]

ual plot graph should be approximately linear in relation to the threshold when the GPD provides a valid approximation.

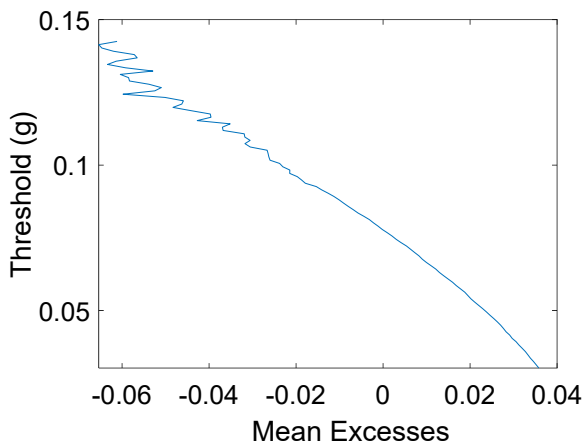


FIGURE 7: THE MEAN EXCESSES OF THE THRESHOLD WITH RESPECT TO THRESHOLD SELECTION FOR NACELLE ACCELERATIONS IN THE FORE-AFT DIRECTION

Figures 7 and 8 show good linearity in certain regions of the graph. This is indicative of the GPD being a good fit for values of that threshold. In both instances, linearity begins to fall off at threshold values of around 0.1. Therefore, a threshold of 0.1 was selected as being an appropriate threshold value to give good results. For both, the analysis does not go below the mean of the data set. As such, the mean of the data set was taken to be μ_0 .

Increasing the threshold to 0.1 ensures that the GPD will still be a good fit, but the results are more indicative of the extreme values of the distribution (Figure 9).

4.3 Generalised Pareto Distribution

MATLAB’s inbuilt ‘Distribution Fitter’ was used to fit the GPD to the data, inputting the threshold determined by Section 4.2. The choice of GPD for this work has been outlined in

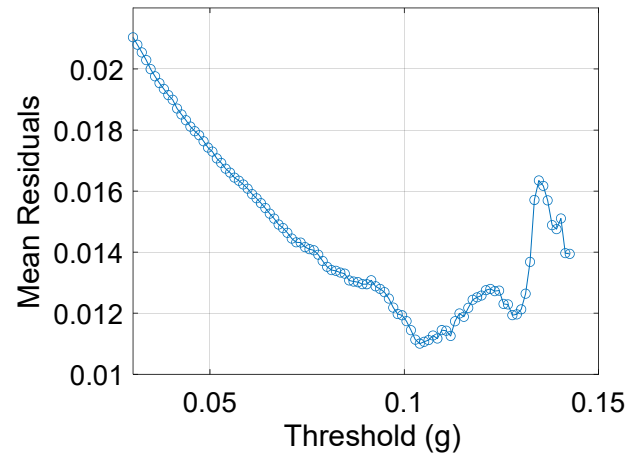


FIGURE 8: THE MEAN RESIDUAL LIFE PLOT OF NACELLE ACCELERATIONS IN THE FORE-AFT DIRECTION

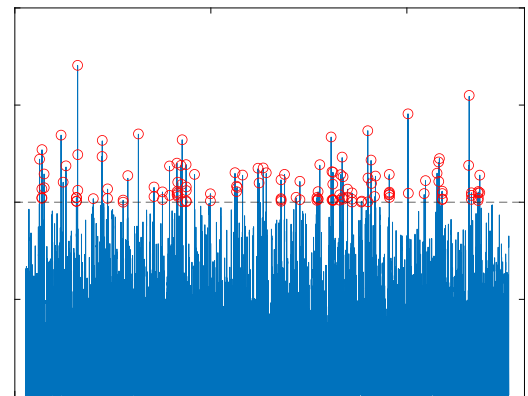


FIGURE 9: POT GRAPH WITH OPTIMISED THRESHOLD SELECTION

Section 3.1. The ‘Distribution Fitter’ uses the MATLAB function “gpdfit” to determine the scale and shape parameter from the data [30]. This function assumes that a threshold has already been fit to the data and the points in the data set have already been chosen. The function returns the maximum likelihood estimates of the parameters in the distribution with the first output generated being the shape parameter and the second output being the scale parameter.

In Figure 10, the fit is shown with the empirical data represented in purple, and the distribution of best fit is represented by the red. In the graphs shown, the empirical dataset represents the exceedances only. The GPD shows that with the selected threshold, most of the extreme values, are covered by the distribution. Statistical plots are a graphical technique used to indicate whether a data set follows a given distribution, and similarly for quantile-quantile plots. As shown, most of the data points lie close to or on the line. This indicates that the method works well

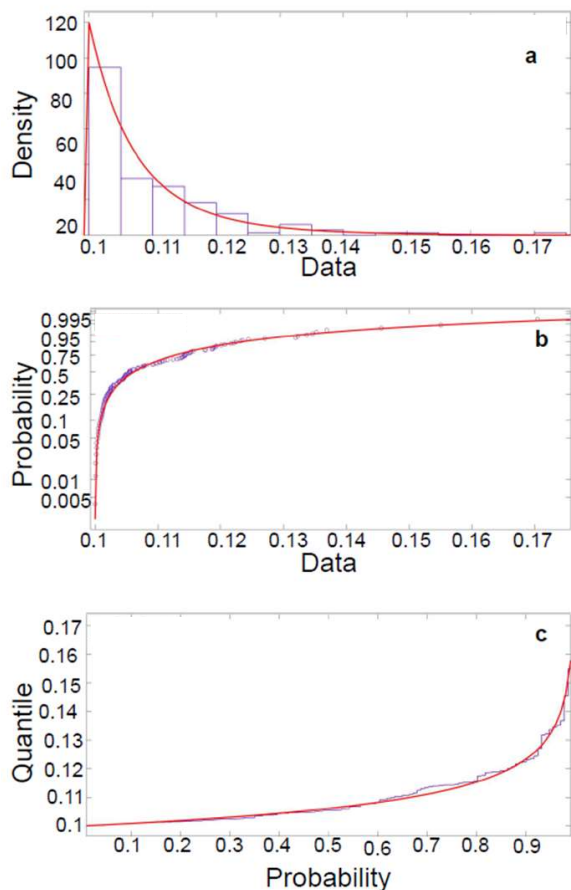


FIGURE 10: THE PROBABILITY DENSITY FUNCTION (PDF) (A), THE CUMULATIVE DENSITY FUNCTION (CDF) (B) AND THE RESIDUAL QUANTILE PLOT (C) OF THE DATA SET FIT TO THE GPD

for fitting a data set to a GPD and thus the GPD is appropriate for use and the method should give meaningful results.

The return value that has been calculated for this threshold is 0.195 g. This is below the standard safety threshold of 0.2 - 0.4 g that nacelle accelerations should remain under and compares well with the maximum recorded nacelle acceleration in the data set of 0.170 g. As acceleration scales 1:1, the full-scale model would experience the same magnitude of accelerations as at model scale.

This value says that in a seastate that comes once every 50 years, the most likely extreme nacelle acceleration that will be found is 0.195 g for this particular sea state and floating wind turbine topology.

5. CONCLUSIONS

In this work, a tank testing programme has been designed to obtain nacelle accelerations from a 1:100 scale model of the reference IEA 15 MW turbine with the Voltturn-US semi-submersible. The work was carried out at the Curved Wave Tank facility in the University of Edinburgh. Using the data obtained, a methodology has been outlined to obtain the most likely extreme nacelle acceleration from a 50 year return period sea state using the POT method and fitting a GPD to the data. A key parameter is the

determination of the threshold which in this case, was selected using previous methods outlined by Coles [22] and was taken to be 0.1 g. The most likely extreme nacelle acceleration for the 50-year return period that has been estimated to be 0.195 g. By exploring the extreme value statistics of nacelle accelerations, the reader can understand the likelihood that the nacelle will exceed limits that could in turn be damaging to the drive train of the offshore floating wind turbine, and may cause fatigue and damage further down the line.

6. FUTURE WORK

The work presented in this paper provides a workable tool to obtain the most extreme value of nacelle accelerations from tank testing results, however, is not an optimised solution. Threshold selection could be further optimised, as well as choice of probability model further explored by comparing dataset values with other probability models such as the GEV. This work is a demonstration of the methodology and there is opportunity for future work to expand upon its findings, such as developing appropriate test plans to ensure there is enough data, and to explore different sea states. The present work only considers the hydrodynamics and is designed to be a methodology that can be applied regardless of the detail of the study. The work could be repeated with multiple different seeds of the sea state. Other considerations for future work would be analysing the effectiveness of using an accelerometer versus qualisys, and performing these tests with aerodynamic loading. This analysis could also be compared with numerical tools such as OpenFAST. Parameters such as tower stiffness could be investigated to determine the impact on the nacelle acceleration outputs with varying tower stiffness. When using scaled models, there are logistical trade-offs, and it would be interesting to explore the impact of nacelle accelerations from these initial design trade-offs, including choice of scale. This would allow a deeper understanding for how accurate nacelle accelerations can be from scaled model testing.

ACKNOWLEDGMENTS

This work was funded by UK Research and Innovation as part of the EPSRC and NERC Industrial CDT for Offshore Renewable Energy (IDCORE). Grant number EP/S023933/1. I would like to acknowledge Katie Smith for the mooring design of the model and Callum Guy and Martyn Lennon at FloWave for the design and assembly of the 1:100 scaled model used in this work.

REFERENCES

- [1] Sebastian, Thomas and Lackner, Matthew A. "Characterization of the unsteady aerodynamics of offshore floating wind turbines." *Wind Energy* Vol. 16 No. 3 (2013): pp. 339–352. DOI [10.1002/we.545](https://doi.org/10.1002/we.545).
- [2] Alkhalidi, Ammar, Kaylani, Hazem and Alawawdeh, Nouredine. "Technology Assessment of Offshore Wind Turbines: Floating Platforms – Validated by Case Study." *Results in Engineering* Vol. 17 (2023). DOI [10.1016/j.rineng.2022.100831](https://doi.org/10.1016/j.rineng.2022.100831).
- [3] Otter, Aldert, Murphy, Jimmy, Pakrashi, Vikram, Robertson, Amy and Desmond, Cian. "A review of modelling

- techniques for floating offshore wind turbines.” (2022). DOI [10.1002/we.2701](https://doi.org/10.1002/we.2701).
- [4] Robertson, Amy, Bachynski, Erin E., Gueydon, Sebastien, Wendt, Fabian and Schünemann, Paul. “Total experimental uncertainty in hydrodynamic testing of a semisubmersible wind turbine, considering numerical propagation of systematic uncertainty.” *Ocean Engineering* Vol. 195 (2020). DOI [10.1016/j.oceaneng.2019.106605](https://doi.org/10.1016/j.oceaneng.2019.106605).
- [5] Mo, John P.T., Cheung, Sherman C.P. and Das, Raj. “Wind Power and Aerodynamics Systems.” *Demystifying Numerical Models*. Elsevier (2019): pp. 33–60. DOI [10.1016/B978-0-08-100975-8.00003-5](https://doi.org/10.1016/B978-0-08-100975-8.00003-5).
- [6] Sirois, Frédéric and Grilli, Francesco. “Potential and limits of numerical modelling for supporting the development of HTS devices.” *Superconductor Science and Technology* Vol. 28 No. 4 (2015): pp. 1–29. DOI [10.1088/0953-2048/28/4/043002](https://doi.org/10.1088/0953-2048/28/4/043002).
- [7] Tracy and Tracy, Christopher H. “Parametric Design of Floating Wind Turbines.” Technical report no. 2007.
- [8] Taboada, Miguel, Ortega, Álvaro, Martín, Rafael, Pombo, Albino, Moreu, Jaime and SI, Seaplace. “An Evaluation of the Effect that Motions at the Nacelle have on the Cost of Floating Offshore Wind Turbines.” 2020. Offshore Technology Conference.
- [9] Nejad, Amir R., Bachynski, Erin E. and Moan, Torgeir. “Effect of axial acceleration on drivetrain responses in a spar-type floating wind turbine.” *Journal of Offshore Mechanics and Arctic Engineering* Vol. 141 No. 3 (2019). DOI [10.1115/1.4041996](https://doi.org/10.1115/1.4041996).
- [10] Allen, Christopher, Viselli, Anthony, Dagher Andrew Goupee, Habib, Gaertner, Evan, Abbas, Nikhar, Hall, Matthew and Barter, Garrett. “Definition of the UMaine VoltturnUS-S Reference Platform Developed for the IEA Wind 15-Megawatt Offshore Reference Wind Turbine Technical Report.” Technical report no. 2020. URL www.nrel.gov/publications.
- [11] Smith, Katie, Davey, Thomas, Forehand, David, Pillai, Ajit C., Tao, Longbin and Xiao, Qing. “Dynamic response of floating offshore renewable energy devices: Sensitivity to mooring rope stiffness.” (2023).
- [12] BSI Standards Publication. *Wind energy generation systems Part 3-1: Design requirements for fixed offshore wind turbines* (2020).
- [13] Bureau of Shipping, American. “Guide for Building and Classing Floating Offshore Wind Turbines 2020.” Technical report no. 2020.
- [14] Davenport, Alan Garnett. “Note on the Distribution of the Largest Value of a Random Function With Application to Gust Loading.” Technical report no. 1964.
- [15] Nolde, Natalia and Zhou, Chen. “Annual Review of Statistics and Its Application Extreme Value Analysis for Financial Risk Management.” (2021)DOI [10.1146/annurev-statistics-042720](https://doi.org/10.1146/annurev-statistics-042720). URL <https://doi.org/10.1146/annurev-statistics-042720>.
- [16] Pedretti, Daniele and Irannezhad, Masoud. “Non-stationary peaks-over-threshold analysis of extreme precipitation events in Finland, 1961–2016.” *International Journal of Climatology* Vol. 39 No. 2 (2019): pp. 1128–1143. DOI [10.1002/joc.5867](https://doi.org/10.1002/joc.5867).
- [17] Kiran, K. G. and Srinivas, V. V. “A Mahalanobis Distance-Based Automatic Threshold Selection Method for Peaks Over Threshold Model.” *Water Resources Research* Vol. 57 No. 1 (2021). DOI [10.1029/2020WR027534](https://doi.org/10.1029/2020WR027534).
- [18] Viselli, Anthony M., Forristall, George Z., Pearce, Bryan R. and Dagher, Habib J. “Estimation of extreme wave and wind design parameters for offshore wind turbines in the Gulf of Maine using a POT method.” *Ocean Engineering* Vol. 104 (2015): pp. 649–658. DOI [10.1016/j.oceaneng.2015.04.086](https://doi.org/10.1016/j.oceaneng.2015.04.086).
- [19] Mackay, Ed, de Hauteclouque, Guillaume, Vanem, Erik and Jonathan, Philip. “The effect of serial correlation in environmental conditions on estimates of extreme events.” *Ocean Engineering* Vol. 242 (2021). DOI [10.1016/j.oceaneng.2021.110092](https://doi.org/10.1016/j.oceaneng.2021.110092).
- [20] Davison, A C and Smith, R L. “Models for Exceedances over High Thresholds.” Technical Report No. 3. 1990.
- [21] Shi, Huanyu, Dong, Zhibao, Xiao, Nan and Huang, Qinni. “Wind Speed Distributions Used in Wind Energy Assessment: A Review.” (2021). DOI [10.3389/fenrg.2021.769920](https://doi.org/10.3389/fenrg.2021.769920).
- [22] Coles, Stuart. *An Introduction to Statistical Modeling of Extreme Values*. Springer London, London (2001). DOI [10.1007/978-1-4471-3675-0](https://doi.org/10.1007/978-1-4471-3675-0).
- [23] Burton, Tony, Sharpe, David, Jenkins, Nick and Bossanyi, Ervin. *Wind Energy Handbook* (2001).
- [24] Far, Soheil Saeed, Wahab, Ahmad Khairi Abd and Harun, Sobri Bin. “Determination of Significant Wave Height Offshore of the Federal Territory of Labuan (Malaysia) Using Generalized Pareto Distribution Method.” *Journal of Coastal Research* Vol. 34 No. 4 (2018): pp. 892–899. DOI [10.2112/JCOASTRES-D-17-00001.1](https://doi.org/10.2112/JCOASTRES-D-17-00001.1).
- [25] Wang, Yingguang. “Optimal threshold selection in the POT method for extreme value prediction of the dynamic responses of a Spar-type floating wind turbine.” *Ocean Engineering* Vol. 134 (2017): pp. 119–128. DOI [10.1016/j.oceaneng.2017.02.029](https://doi.org/10.1016/j.oceaneng.2017.02.029).
- [26] Wilson, Amy L and Zachary, Stan. “Using extreme value theory for the estimation of risk metrics for capacity adequacy assessment.” (2019)URL <http://arxiv.org/abs/1907.13050>.
- [27] Moriarty, P J, Holley, W E and Butterfield, S P. “Extrapolation of Extreme and Fatigue Loads Using Probabilistic Methods.” Technical report no. 2004. URL <http://www.osti.gov/bridge>.
- [28] Agarwal, Puneet and Manuel, Lance. “Simulation of offshore wind turbine response for long-term extreme load prediction.” *Engineering Structures* Vol. 31 No. 10 (2009): pp. 2236–2246. DOI [10.1016/j.engstruct.2009.04.002](https://doi.org/10.1016/j.engstruct.2009.04.002).
- [29] MathWorksR2023b. “findpeaks - Find local maxima.” (2023).
- [30] MathWorksR2023b. “gpfitt - Generalized parameter estimates.” (2023).